International Journal of Mass Spectrometry 294 (2010) 7–15

Contents lists available at ScienceDirect

International Journal of Mass Spectrometry

journal homepage: www.elsevier.com/locate/ijms

Laser spot size and laser power dependence of ion formation in high resolution MALDI imaging

Sabine Guenther, Martin Koestler, Oliver Schulz, Bernhard Spengler*

Justus Liebig University, Analytical Chemistry, Giessen, Germany

ARTICLE INFO

Article history:
Received 30 July 2009
Received in revised form 31 March 2010
Accepted 31 March 2010
Available online 8 April 2010

Keywords:
MALDI
Laser spot area
Laser beam profile
Laser fluence
Desorption
Ionization

ABSTRACT

Laser focus diameters (optical resolution) and dependence of ion signal intensities on laser fluence were investigated for MALDI imaging mass spectrometry at high spatial resolution (optical focus diameters in the range of 1.1–8.4 μm). Results are of interest in the light of MALDI mechanisms and of methodological optimization, since no data was available yet for such small laser spots. The dependence of ion signal intensities on laser fluence was found to be in line with data published for larger laser spot diameters. Results argue for a common general mechanism in MALDI, with a steady trend of parameter values when going from larger (>100 μm) to smaller (<10 μm) spot sizes.

1. Introduction

Since the introduction of matrix-assisted laser desorption/ionization (MALDI) in 1985–1987 [1–4] there has been a constant interest in understanding its underlying mechanisms. Especially in the light of the development of MALDI imaging [5,6], mechanisms of ion formation and their relation to laser focus parameters are central questions in all attempts of optimizing the method. Among the influencing factors are laser parameters such as irradiated area, wavelength and laser pulse energy, sample properties such as substance concentration, morphology and matrix used and the design of the mass spectrometer including ion source geometry, residual gas pressure, mass analyzer type and detector type. Due to the complexity and partial inconsistency of the experimental results no generally accepted, comprehensive and universal model of MALDI mechanisms has been proposed yet.

Nevertheless a number of basic properties are well-known and described for MALDI. Firstly, highest analyte ion signal intensities are achieved when the laser wavelength matches the absorption maximum of the used matrix [3,7–10]. Secondly, a minimum laser fluence is necessary to achieve analyte ion signals with a sufficient signal-to-noise ratio [11,12]. This so called threshold fluence for ion detection appears to be a parameter defined by instrumental limits of detection (LOD) rather than by a real substance specific and mechanistically defined physical threshold [13]. For a given instrumental LOD and a given sample the threshold fluence is known to increase with decreasing laser spot area [11,14]. Dreisewerd et al. have reported that for a fixed laser fluence the dependence of ion signal intensities on area is described by a cube function A^3 for laser focus diameters between 200 and 10 μm [11], later confirmed by Qiao et al. [12]. More important for practical work is the behavior with varying fluence for a given spot size. Above threshold fluence ion signal intensities are generally found to increase rapidly with fluence, until saturation of ion signal intensities takes place [15]. Saturation is understood to be due to the prevalence of secondary processes such as ion fragmentation. The dependence of ion signal intensities on laser fluence is often described by the power function $I \propto H^m$ (I ion signal; H fluence). The values of m as well as the dynamic range of ion signal intensities decrease with decreasing laser spot size [11]. Thirdly, the laser pulse duration has only a minor effect on the ion signal intensities within the pulse duration regime typically used for UV-MALDI (0.3–20 ns) [16,17].

MALDI Imaging was introduced as a Scanning Microprobe Matrix Assisted Laser Desorption/Ionization Mass Spectrometry (SMALDI-MS) method in 1994 [5]. SMALDI-MS is a MALDI imaging method which features the possibility to investigate and visualize the spatial distribution of analytes in samples with sub-cellular resolution (0.5–10 μm) [5,6]. A detailed characterization of spatial resolution and performance at such small laser focus size was still lacking. Extrapolating the published desorption model (derived for spots sizes between 200 and 10 μm) [11] down to the sub-micrometer regime of the SMALDI method would predict undetectability of ion signals, in sharp contrast to reality in everyday experimental results. It was therefore necessary to inves-

* Corresponding author.
E-mail address: Bernhard.Spengler@anorg.Chemie.uni-giessen.de (B. Spengler).

1387-3806/$ – see front matter © 2010 Elsevier B.V. All rights reserved.
doi:10.1016/j.ijms.2010.03.014

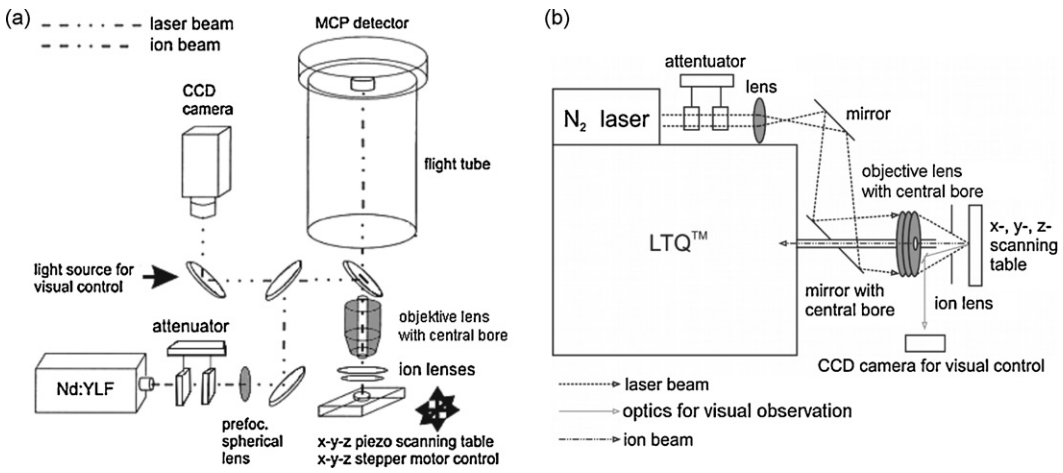

Fig. 1. Scheme of the instrumental setup: (a) SMALDI time-of-flight instrument "LAMMA 2000", (b) AP-SMALDI ion source connected to a linear ion trap (LTQ ™, Thermo Scientific GmbH, Bremen).

tigate laser focusing parameters and ion formation behavior at low-micrometer and sub-micrometer spot sizes in order to understand and further improve high resolution MALDI imaging.

2. Experimental

2.1. Instrumental setup

Two different SMALDI mass spectrometers were employed. One was the home-built LAMMA 2000 instrument [2]. As a time-of-flight instrument it was equipped with a Nd:YLF solid state laser (diode-pumped, Q-switched frequency-tripled laser, Triton, Spectra Physics, Stahnsdorf, Germany, $\lambda = 349$ nm, pulse duration <15 ns, divergence = 1.1 mrad) for desorption/ionization. Desorption/ionization and ion transmission took place under high vacuum conditions (1×10^{-6} mbar). The time-of-flight mass analyzer was equipped with a microchannel plate detector (Tectra, Frankfurt, Germany). Mass spectra were acquired, displayed and analyzed by the data-acquisition software Ulisses 8.21 [18].

The second instrument was a new atmospheric pressure SMALDI mass spectrometer (AP-SMALDI-LTQ) [19]. It consisted of a home-built atmospheric pressure SMALDI ion source, connected to a commercial linear ion trap mass spectrometer (LTQ™, Thermo Scientific GmbH, Bremen, Germany). The instrument was equipped with a secondary electron multiplier as an ion detector. Desorption/ionization was initiated by a nitrogen laser (MNL202-LD, LTB, Berlin, Germany, $\lambda = 337$ nm, pulse duration = 800 ps, divergence = 1.7 × 1.2 mrad). Mass spectra were acquired, displayed and analyzed by the instrument software (Tune Plus 1.0 and Xcalibur 1.4 Thermo Scientific GmbH, Bremen, Germany).

Except for the above-mentioned differences in instrumental setup the optical design of both instruments was very similar. Focusing the laser beam down to a few micrometers required a dedicated optical setup. A normal incidence of laser light onto the sample was mandatory to obtain a circular focus and an optimal and constant ion transmission [20,21]. Therefore the laser beam first passed an attenuator, controlling the laser pulse energy. The attenuator consisted of two rotatable dielectrically coated quartz plates. The transmission of the coated quartz plates depended on the angle of incident light. The laser pulse energy was set by counterrotation of the two plates. After passing the attenuator the laser beam was focused by a pre-focusing lens (focal length 25 mm) to a diameter of 15–30 μm. The divergent laser beam was then reflected by several mirrors into the back entrance of a specially designed objective lens, which focused the laser beam to the final size. The complete beam path was optimized to keep the beam quality as close as possible to the diffraction limit. Besides optimized focusing the optical setup featured a coaxial alignment of laser beam and ion beam for highest ion transmission efficiency into the mass spectrometer. To achieve this alignment both, the objective lens and the following mirror exhibited central bores, which covered a stainless steel tube for ion transfer into the mass spectrometer. The total optical transmission of the complete optical setup (laser exit to sample plane) of the LAMMA 2000 instrument with the attenuator in lowest absorption position was determined as 1.5%. The optical transmission of the AP-SMALDI source under the same conditions was determined as 15%. Transmission losses of the two setups are mainly due to the loss of laser energy through the central bores of the focusing objectives and mirrors. A scheme of the two mass spectrometers is shown in Fig. 1.

2.2. Determination of laser beam profile and dimensions

For determination of laser beam profiles and dimensions an interlaced frame transfer CCD camera 4812 (Cohu, Inc., San Diego, CA, USA) was used in combination with laser beam analyzer software LBA-7XXPC (Spiricon Inc., Logan, USA). Since the camera pixel size of 27.0 μm (h) × 27.0 μm (v) was too large for analysis of very small laser beams (<10 μm in diameter), two UV microscope objective lenses (Ultrafluar 32× or Ultrafluar 100×, Carl Zeiss AG,

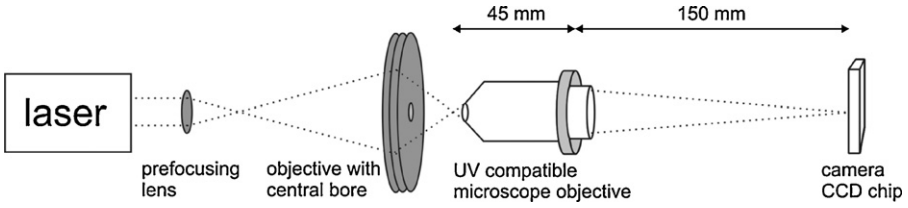

Fig. 2. Setup for micro-optical imaging of the laser beam focus.

Oberkochen, Germany) were added to the setup in front of the camera chip for alternative magnification of the laser beam. In order to stay within a sufficient ratio of focus size and camera pixel size, the Ultrafluar 32× was used for measurements on the AP-SMALDI ion source, while the Ultrafluar 100× was used for measurements on the LAMMA 2000 setup. The assigned magnification of the microscope objectives (32× and 100×) was achieved with a distance of 150 mm between camera chip and microscope objective mounting (nosepiece opening) (Fig. 2).

The working distance of the microscope objective was 45 mm, measured from the nosepiece opening of the objective to the focal plane. For objectives Ultrafluar 32× and Ultrafluar 100×, the distances between focus and objective entrance thus were 0.8 and 0.42 mm, respectively. The dynamic range of the camera chip was 0.01–3 nJ/cm^2. Additional neutral-density filters (Spindler & Hoyer GmbH, Göttingen, Germany) were used for attenuation of the laser pulse energy during measurements. Analog to digital conversion was performed by a 14 bit frame grabber card. Processing and display of data was performed by the software LBA-7XXPC. For optimal adjustment of the setup to the laser beam axis and for precise investigation of the laser beam dimensions along the optical axis of the laser beam, both microscope objective and CCD camera were mounted on a micrometer stage and were movable in three dimensions with accuracies in the range of 5 μm. The quality of the magnification system was tested by imaging of known test structures (electron microscopy grids, apertures) which were positioned in the focal plane. The assigned magnification of the microscope objectives (32× and 100×) was confirmed with an uncertainty of ±1. The optical quality of the magnification setup (commercial UV microscope objective, Zeiss) and numerical aperture were higher than the expected quality and numerical aperture of the mass spectrometer's optical setup. No deterioration of the optical focusing conditions by magnification was thus expected.

Calculations of laser beam diameters were based on the $1/e^2$ definition, where e is Euler's number, and the boundaries of the laser beam are defined at $1/e^2$ (≈13.5%) of the peak intensity [22] (Supplementary Fig. 1a). The focal plane of the SMALDI optical setup was determined by measuring the laser beam diameter at various positions along its beam waist behind the objective. The range which was investigated along the beam waist of the focused laser beam depended on dynamic range of the CCD camera and divergence of the focused laser beam. For the LAMMA 2000 setup the measurement range was smaller than for the AP-SMALDI ion source. Within this measurement range the peak intensity of the laser beam varied by more than 70%. At each position along the beam waist 50 laser beam profiles, acquired from 50 laser pulses, were measured. Afterwards mean value and standard deviation were calculated from the diameters of the 50 laser beam profiles. Each beam waist was measured three times. The position along the beam waist, where mean laser beam diameter was the smallest, was taken as the "focus position" (Supplementary Fig. 1b). Its mean laser beam diameter was taken as the "optical focus diameter".

2.3. Laser pulse energy

The total laser pulse energy was examined by an energy measurement system purchased from Coherent GmbH (Dieburg, Germany), consisting of an energy sensor J10MB-LE, an energy meter FieldMaxII TOP and a dedicated software package. The accuracy of the total laser pulse energy determination system was better than ±7%. The total laser pulse energy on the target was determined as a function of the angle of the attenuator quartz plates. At each position of the attenuator a mean energy value and a standard deviation were determined from the pulse energies of 100 laser pulses. As a result of pulse-to-pulse energy fluctuations of the laser (±3% for both lasers) the overall accuracy of the calculated mean pulse energy was within ±10% for both instruments.

Table 1
Terms and definitions of parameters as used in this paper.

Term	Definition
Focus position	Position along the beam waist, where the mean laser beam diameter was the smallest
Optical focus diameter	Mean laser beam diameter determined by $1/e^2$ definition at the focus position
Optical focus area	Area within the $1/e^2$ intensity boundaries of the laser focus
Detection threshold	Signal-to-noise ratio for the ion of interest is 2:1 or better in 50% of the collected mass spectra
(Threshold) pulse energy	Total laser pulse energy on the target (required to reach the detection threshold)
(Threshold) focus energy	Laser pulse energy within the optical focus area (required to reach the detection threshold)
(Threshold) focus fluence	Focus energy (required to reach the detection threshold) per optical focus area
Peak fluence	Maximum fluence within the optical focus area

2.4. Sample preparation

Sample solutions were prepared by mixing a solution of 2,5-dihydroxybenzoic acid (1.5×10^{-1} mol/l; purchased from Fluka, Buchs, Switzerland) in 1:1 (v/v) ethanol/water with a solution of the neuropeptide Substance P (2×10^{-4} mol/l; purchased from Sigma, Munich, Germany) in the same solvent in a volume ratio of 4:1. Since ion signal intensities in MALDI-MS are strongly influenced by the preparation technique and by the size of the matrix crystals, a homogeneous distribution of analyte on the target and uniform crystal sizes of matrix was intended [23], in order to obtain ion signal intensities depending solely on laser parameters and mass spectrometer properties rather than on sample preparation inhomogeneities. Therefore sample solutions were applied to a gold-coated aluminum target by pneumatically assisted spray deposition. With this preparation technique a uniform crystal layer was achieved, covering the complete target with an averaged thickness of approximately 3 μm and crystal sizes between 1 and 10 μm. Light microscopic images of the prepared MALDI sample surfaces are given in the Supplementary Fig. 2.

2.5. Mass spectra – data acquisition

All measured mass spectra were single laser pulse acquisitions. Since highest ion signal intensities and highest spatial resolution are expected with the sample situated in the focal plane of the optical setup, much care was taken in positioning the sample. Therefore the laser pulse energy was decreased stepwise, so that the region along the optical axis of the laser beam, within which the energy density was sufficient for ion generation, diminished stepwise until only one position was left, from which ion generation occurred. Ion signals considered for sample positioning and for the following investigations were those of the averaged and the monoisotopic $[M+H]^+$ signal of Substance P, which appear at $m/z = 1348.7$ and $m/z = 1347.7$, respectively. The averaged $[M+H]^+$ signal of Substance P was used for measurements with the LAMMA2000 instrument in the linear detection mode, due to its lower mass resolving power.

A number of definitions are listed in Table 1 to clarify terms used in the following discussion. The "optical focus area" was defined by us as the area within the $1/e^2$ intensity boundaries of the laser focus. By definition, the detection threshold for an ion of inter-

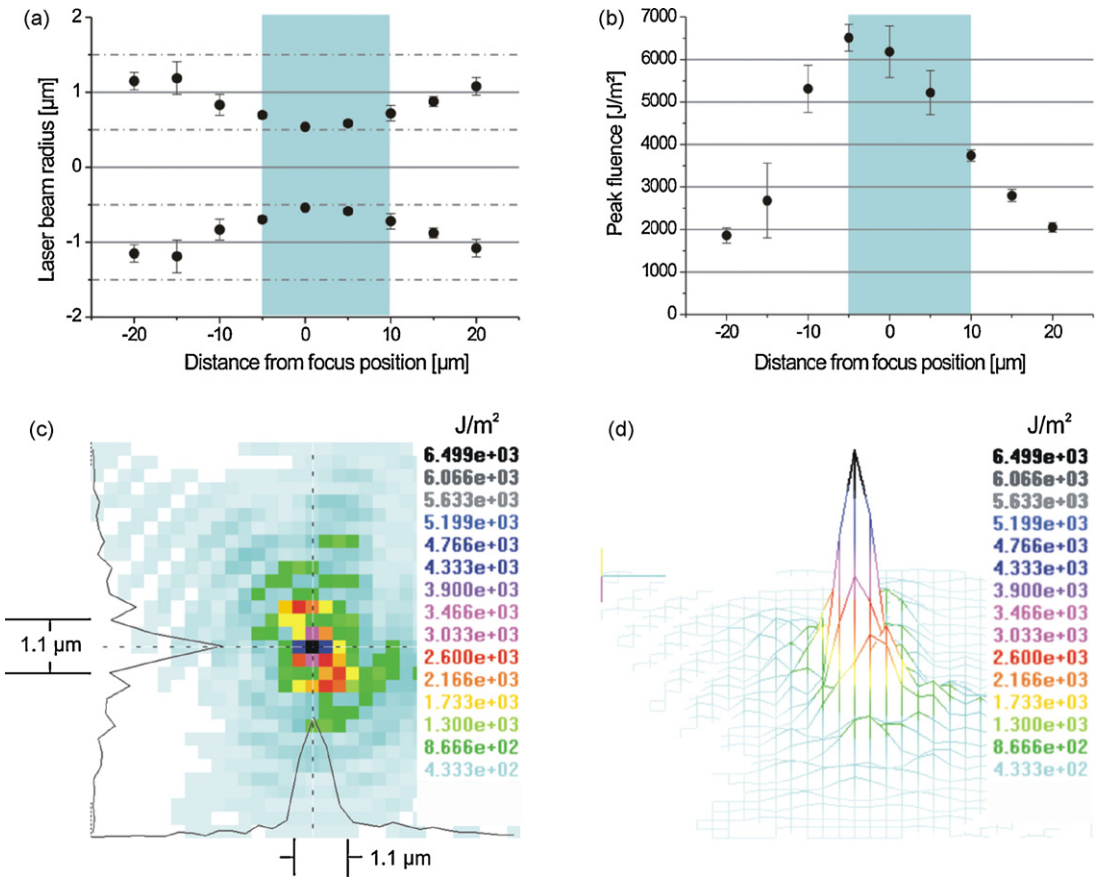

Fig. 3. Laser focus of LAMMA 2000 SMALDI ion source; (a) beam waist formed by focusing the laser beam by the objective into the sample plane of the mass spectrometer. Laser beam radius values were mirrored to illustrate the shape of the beam waist. Negative distances from focus position correspond to positions between objective and its focal plane. The shaded area shows the focal depth. (b) Distribution of peak fluences along the beam waist. (c) and (d) 2D and 3D images of the laser beam profile. Laser beam energies per pixel area are displayed as color bar. Total laser pulse energy was twice the threshold energy required for ion detection.

est was regarded as being reached, when the signal-to-noise ratio in 50% of the collected spectra was 2:1 or better. The total laser pulse energy, required on target to reach the detection threshold was defined as "threshold pulse energy". The share of that energy located within the optical focus area was defined as "threshold focus energy". This energy divided by the optical focus area on the sample was termed "threshold focus fluence". Since the laser beam has a near-Gaussian beam shape the focus fluence represents a value averaged across the optical focus area, with local fluence values higher or lower than the threshold focus fluence. The "peak fluence" instead was defined as the maximum fluence within the optical focus area, as determined by the camera system with camera pixel resolution.

For determination of threshold focus fluences, a number of 50 single shot spectra per selected laser pulse energy was collected and analyzed. Each spectrum was taken from a new sample position to avoid ion signal variations due to sample consumption and to statistically minimize the influence of sample preparation artifacts.

Above threshold focus fluence (i.e., at higher signal-to-noise ratio), the influence of laser pulse energy on ion signal intensity was determined by acquiring and analyzing 15 spectra per selected laser pulse energy. The signal intensity of an ion of interest was determined by peak integration from each spectrum. Mean value and standard deviation were determined for each selected laser pulse energy. For a better comparability between instruments the ion signal intensity at threshold focus fluence was normalized to 1.0 for the two mass spectrometers.

3. Results

3.1. Optical resolution

3.1.1. LAMMA 2000 SMALDI source

The measured beam waist of the laser beam in the sample plane of the LAMMA 2000 instrument is shown in Fig. 3a.

Although a considerable part of the laser beam's center energy was lost due to axial perforation of objective lens and mirror, its beam waist after focusing by the objective lens exhibited an almost perfect profile with only slight asymmetry of the branches. The laser beam diameter determined at the focus position (i.e., the "optical focus diameter") was 1.1 ± 0.3 µm. The focal depth is defined by the range along the beam axis in which the laser beam diameter increases by a factor of <1.41 ($\sqrt{2}$) of the optical focus diameter [22]. For the LAMMA 2000 setup it was determined as 15 µm. Within the focal depth the peak fluence of the laser beam profile decreased to about 50% with increasing distance from the focal point (Fig. 3b). So the region along the beam waist, where ion generation occurs, is expected to be small, too. The effect that the highest peak fluence appears at a distance of −5 µm from the focal plane is most probably an experimental artifact within the displayed measurement errors. An averaged laser beam profile at the focal plane is shown in Fig. 3c and d. It was acquired from 50 single laser pulses. The overall structure of the laser beam profile is caused by diffraction. The determined focal spot size is related to the central maximum of the diffraction pattern, which exhibits a near-Gaussian beam shape. About 83% of the total laser pulse

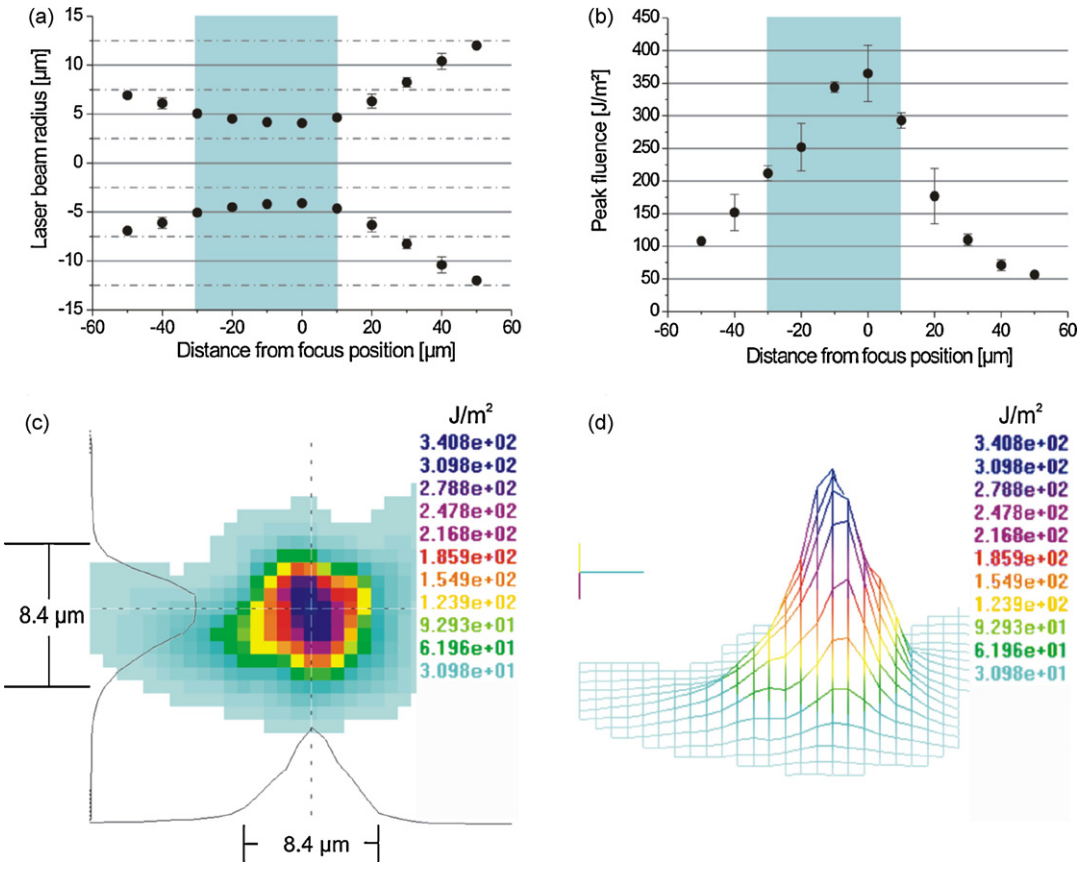

Fig. 4. Laser focus of the AP-SMALDI setup on the LTQ linear ion trap; (a) beam waist formed by focusing the laser beam by the objective into the sample plane of the mass spectrometer. Laser beam radius values were mirrored to illustrate the shape of the beam waist. Negative distances from focus position correspond to positions between objective and its focal plane. The shaded area shows the focal depth. (b) Distribution of peak fluences along the beam waist. (c) and (d) 2D and 3D images of the laser beam profile. Laser beam energies per pixel area are displayed as color bar. Total laser pulse energy was twice the threshold energy required for ion detection.

energy was found to be located in the side maxima of the pattern, i.e., outside the central maximum. The fact that the intensities of the side maxima of the pattern are rather high in the LAMMA 2000 setup is due to the stronger influence of the central bore of the objective lens. It is known from other experiments with our setup, however, (especially from MALDI imaging) that these side maxima are ineffective for ion formation. Ion images generated with a step size of 1 µm have sharp edges rather than blurred contours as would be expected if a significant number of ions would stem from larger areas [23,24]. It is furthermore known that ion formation is related to material ablation (rather than evaporation) and thus to burn pattern size [25], which was found to be in the range of 0.6–0.7 µm [6]. It is therefore reasonable to describe the focus size as related to the central maximum only, i.e., related to the area of ion formation.

3.1.2. AP-SMALDI source

Results for the optical system of the AP-SMALDI-LTQ are shown in Fig. 4. The objective lens designed for this setup was a three quartz lens system, compared to the five lens system developed for the LAMMA 2000 objective. In addition the beam quality of the nitrogen laser used for the AP-SMALDI setup was lower than that of the Nd:YLF laser used in the LAMMA 2000 setup. As a result of the lower optical quality of the AP-SMALDI setup, focusing was found to be limited to a minimum optical focus diameter of 8.4 ± 0.8 µm. Focal depth was found to be 40 µm with this setup (Fig. 4a). Within this range the peak fluence of the laser beam profile decreased to about 45% with increasing distance from the focal point (Fig. 4b). The region along the beam waist, where ion generation occurs, is expected to be larger than that of the LAMMA 2000 instrument, due to the larger focal depth (40 µm compared to 15 µm).

A well shaped beam waist was found for the AP-SMALDI setup. An averaged laser beam profile obtained at the focus position is shown in Fig. 4c and d. It was acquired from 50 single laser pulses and exhibited an almost perfect Gaussian beam shape. Only 25% of the total laser pulse energy was found to be located outside the optical focus area.

3.2. Dependence of ion signal on laser fluence

3.2.1. LAMMA 2000 SMALDI source

The threshold pulse energy determined for desorption/ionization and detection of Substance P with the LAMMA 2000 instrument was 11.5 ± 2.8 nJ. At least 83% of this energy was regarded to be ineffective for desorption/ionization due to its location outside the focus area, as described above. The estimated "threshold focus energy" was thus 1.96 ± 0.5 nJ. The "threshold focus fluence" was thus 2062 J/m^2. Dependence of the Substance P ion signal intensity on laser focus fluence is shown in Fig. 5. Ion signal intensities of Substance P were found to increase by a factor of 32 for an increase of laser focus fluence by a factor of 19, expressing an almost linear power dependence ($m = 1.2$). Focus fluence values above 19 times threshold focus fluence were found to lead to saturation of the ion signal.

3.2.2. AP-SMALDI source

Threshold pulse energy for desorption/ionization and detection of Substance P with the AP-SMALDI-LTQ setup was determined

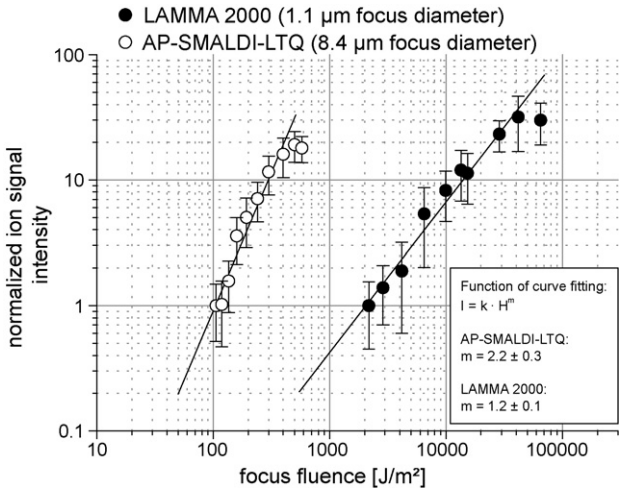

Fig. 5. Dependence of Substance P ion signal intensity ($[M+H]^+$) on laser focus fluence determined for the LAMMA 2000 and the AP-SMALDI-LTQ setup.

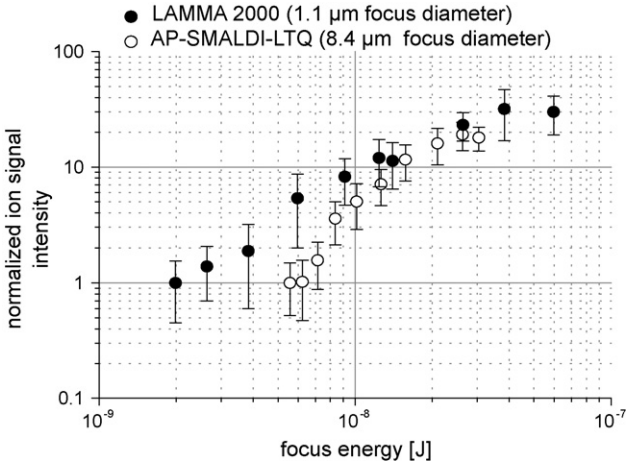

Fig. 7. Dependence of Substance P ion signal on focus energy determined for the LAMMA 2000 and the AP-SMALDI-LTQ setup.

as 7.4 ± 0.8 nJ. Approximately 25% of this energy was regarded to be ineffective for desorption/ionization as being located outside the optical focus area. Corrected threshold focus energy was thus 5.6 ± 0.6 nJ. Corresponding threshold focus fluence was 100 J/m^2.

The dependence of the Substance P ion signal intensity on laser fluence with the AP-SMALDI-LTQ setup is shown in Fig. 5. The ion signal intensity of Substance P increased by a factor of 16 while increasing the laser fluence by a factor of 4 and then saturated. An almost quadratic power dependence of ion signal intensities was thus observed ($m = 2.2$). The threshold focus fluence for desorption/ionization of Substance P as determined with the AP-SMALDI-LTQ setup was found to be by a factor of 21 ± 8 lower than that determined with the LAMMA 2000 setup.

Two mass spectra describing typical conditions of single laser pulse analysis at twofold threshold fluence of ion detection are shown in Fig. 6 for the two mass spectrometers. In both mass spectra the Substance P molecular ion peak is clearly above noise. Within the measured fluence ranges (below saturation) no or only minor fragmentation of analyte ions was observed with both instrumental setups. Since ion detection at the LAMMA 2000 was done in linear TOF mode, only in-source fragmentation was detected. A detailed discussion of mass spectra quality at different laser fluences will be given in a separate paper.

Comparing threshold focus energies of the two instruments, instead of comparing threshold focus fluences interestingly led to rather similar results for the two focusing conditions. Fig. 7 shows the dependence of ion signal intensities on focus energies. Focus energies at 1.1 and 8.4 µm diameter, respectively, were found to differ by a factor of 2.9 at the threshold only and (due to the steeper slope at the larger focus area) were found to become equal (normalized to threshold conditions) under saturation conditions, while the irradiated areas differed by a factor of 61.

4. Discussion

Threshold fluences and dependences of ion signal intensity on laser fluence have been determined previously by several groups for MALDI mass spectrometry [11,12,14,26–28]. Absolute values of threshold fluences and slopes of the ion signal curves show considerable differences in these reports. A number of parameters have been suggested to cause these differences, among them the irradiated area, laser pulse length, laser wavelength and laser beam profile (flat top/Gaussian), sample properties such as substance concentration, morphology and matrix used and the design of the mass spectrometer (ion source geometry, pressure, mass analyzer type, detector type). These parameters vary quite often in individual studies and complicate a proper comparison of results.

Dreisewerd et al. and Qiao et al. performed detailed studies on the impact of irradiated area on ion signal intensities [11,12]. Both covered laser spot sizes ranging from 10 to 200 µm in diameter in their studies. Our measurements extend these investigations towards smaller laser spot sizes, keeping as many parameters as possible similar to the reported ones. Qiao determined a threshold fluence (assumed to be the "threshold focus fluence" according to our definition) of about 180 J/m^2 for a laser spot diameter of 200 µm and of 1600 J/m^2 for a diameter of 10 µm. The slope m in the ion signal versus fluence curve (according to the power func-

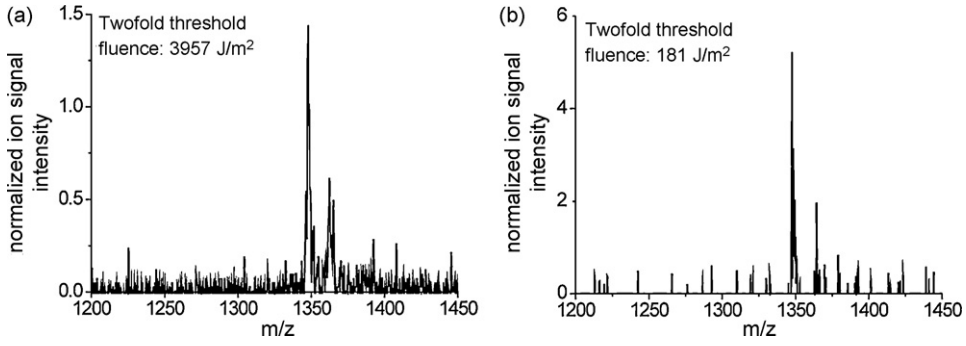

Fig. 6. Typical single laser pulse mass spectra obtained at the twofold threshold fluence of ion detection with: (a) the LAMMA 2000 instrument, (b) the AP-SMALDI-LTQ. Substance P ion signal intensity at threshold fluence was normalized to 1.0 for both mass spectrometers.

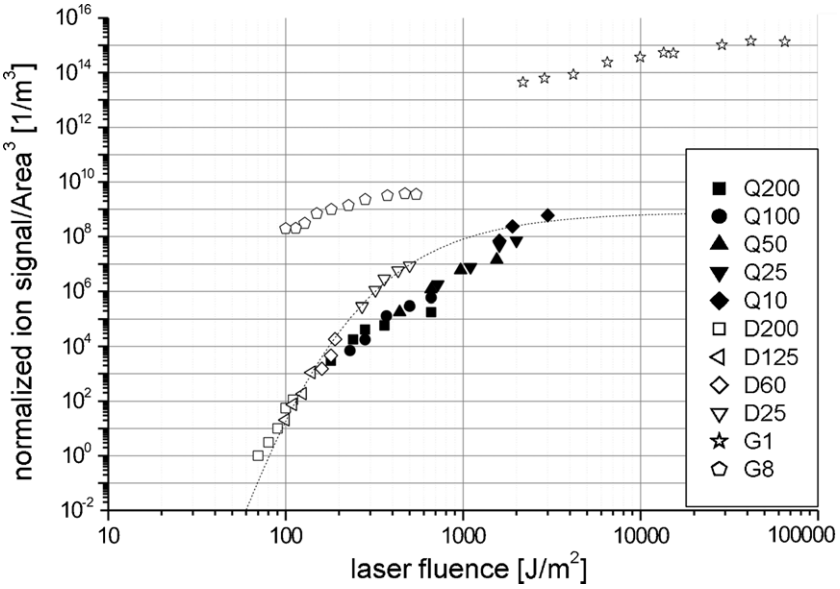

Fig. 8. Comparison of present results described in this paper (G) with results of earlier studies [11,12]. Data labeled (D) were estimated from Fig. 4 in Ref. [11], those labeled (Q) were estimated from Fig. 12(a) in Ref [12]. Data points associated to saturation of the ion signal intensities were omitted. Ion signal intensities were normalized to the lowest detected ion signal intensity for each measurement. Values of ion signal intensities/(area)^3 were normalized to its lowest values for all measurements. The dashed line describes the best fit to the quasi-thermal model proposed by Dreisewerd et al. [11] using their fit parameters E_a = 1.77 eV, η = 8.7 km^2/J and T_0 = 298 K.

tion $I \propto H^m$) was determined as m = 10.5 for a laser spot diameter of 200 μm and as m = 4.5 for a laser diameter of 25 μm [11]. In addition the dynamic range of the ion signal intensities was reported to decrease with decreasing laser spot size from 3 orders of magnitude for a diameter of 200 μm to 2 orders of magnitude for a diameter of 25 μm [11]. Our results for 1.1 and 8.4 μm optical focus diameter appear to follow the same trend. A smaller slope of the ion signal versus fluence curve and a smaller dynamic range of ion signals were observed for our smaller focus spot sizes. The slope m determined for the ion signal versus fluence curve was determined as 2.2 for the AP-SMALDI-LTQ setup and 1.2 for the LAMMA 2000 setup. The dynamic range of ion signal intensities was found to be only about one order of magnitude.

In addition both studies claim that the dependence of ion signal intensity on laser spot area for a given fluence is described by a cube function [11,12]. Qiao showed that the dependence of ion signal intensity per area^3 on fluence is described by a common function for the different laser spot sizes. Dreisewerd supposed a quasi-thermal model to describe this function. In order to compare our results with these findings, the differences in instrumental setup, sample preparation, ambient pressure and measurement conditions were neglected. Data of the earlier measurements [11,12] were divided by the cube of the laser spot area for each laser spot size. Data points located in the ion signal saturation region were omitted. All values were normalized to the lowest measured ion signal intensity in each measurement. Normalization was also performed for the ion signal/(area)^3 values of all data sets for display purposes. Results of this data evaluation are shown in Fig. 8.

At first view, there is no common trend observable for Qiao's, Dreisewerd's and our data. Compared to Oiao's and Dreisewerd's data, our data differ considerably in slope and absolute value. Also the proposed quasi-thermal model with its published parameter values does not fit to our data (Fig. 8 dashed line). It seems that our data show a similar behavior as Oiao's and Dreisewerd's data, but starting at much lower fluences. This does not suggests a general change in MALDI mechanisms at smaller spot sizes, but simply a shift of fluence values caused most likely by different experimental conditions. There are a few factors which probably caused the smaller fluences necessary in our study. Experimental differences like laser wavelength, pulse duration, pressure, ion mass analysis and ion detection certainly influenced the results to some extent. Influences of ion mass analysis principles are mostly unknown so far. Since Dreisewerd's and Qiao's studies were performed under vacuum conditions while our AP-SMALDI-LTQ data were measured at atmospheric pressure, it can be assumed that the observed differences in behavior are influenced by pressure. There is not much data available concerning the dependence of ion signal intensities on laser fluence for different laser spot sizes at atmospheric pressure. On the basis of the published data it appears that threshold laser fluences applied in vacuum MALDI and atmospheric pressure MALDI are similar [29]. On the other hand Doroshenko et al. claim that the total ion yield in an AP-MALDI source is higher than in a vacuum MALDI source [30]. A higher ion yield at atmospheric pressure compared to vacuum conditions might be a reason for the lower threshold fluence values obtained for our AP-SMALDI-LTQ setup.

Differences in laser wavelength are known to contribute only marginally to the effects observed in our case. Horneffer et al. showed that the absorption values of DHB at 337 and 349 nm are similar [8] leading to a comparable desorption/ionization behavior. Influences of laser pulse lengths are expected to be negligible as well, since for all measurements compared here, desorption took place in the regime of thermal confinement. A number of studies described no or only minor differences in threshold fluence by changing the pulse length within this regime [3,16,26].

The laser beam profile certainly has an impact on the results. We employed a Gaussian laser beam profile compared to a flat top profile used by Qiao and Dreisewerd. While an ideal flat top profile has a homogenous fluence distribution, the Gaussian profile has an inhomogeneous distribution of fluences and only a mean value is presented in the diagram. A Gaussian profile with the same optical focus diameter ($1/e^2$) as a flat top profile will therefore require a lower mean fluence value for generating a detectable ion signal, due to higher peak values in the center of the Gaussian profile. Moreover the slope of ion signal versus fluence curve is lower for the measurement done with a Gaussian profile, because the area, from which material is ablated (burn pattern size) increases with increasing laser energy, while it stays the same for a laser beam with flat top

profile. Obviously flat-top profiles cannot be generated under high focusing conditions (under diffraction limited conditions). Implications of Gaussian beam profiles on effective desorption/ablation area are rather complex and will be the topic of a follow-up paper.

Our setup uses coaxial geometry with a laser beam incidence perpendicular to the surface. This might result in a lower threshold fluence compared to the tilted laser incidence used by Qiao et al. and Dreisewerd et al., keeping in mind that coaxial alignment is known to improve ion transmission considerably [21].

Measurements obtained with a similar setup with other matrices point into the same direction [31]. A threshold pulse energy of 3.8 nJ for Substance P in sinapinic acid matrix was determined for a laser spot diameter of 7 μm in a MALDI-TOF system. This is in good agreement with our AP-SMALDI LTQ data. The optical setup of their instrument is almost the same as ours, as both optics and ion sources were designed and built by Spengler. One might conclude from this observation that the benefit of coaxial alignment probably has been underestimated.

Two other parameters of MALDI, the ablation volume and the mass range at laser diameters below 10 μm need to be discussed briefly, even if not a specific topic of this paper. The ablation volume per laser pulse for generation of a usable spectrum (Fig. 6) can be estimated from burn patterns and ablation depth measurements. Volumes were calculated by multiplying burn pattern area and sample thickness (3 μm) divided by the number of laser pulses necessary for a complete ablation of the sample. An ablation volume of about 0.4 μm^3 was estimated at 1.1 μm focus diameter (LAMMA 2000) and one of 0.7 μm^3 at 8.4 μm focus diameter (AP-SMALDI-LTQ). Such values of ablation volume are considerably smaller than those estimated for standard MALDI analyses (approximately 8μm^3 at 100 μm focus diameter and 1 nm ablation depth). The spatial sensitivity (ion signal/volume and ion signal/area) is thus significantly higher for small laser spot sizes. This finding is in good agreement with an increase in sensitivity with decreasing laser spot size as observed by Qiao et al.

The mass range of the AP-SMALDI LTQ system is limited to 4000 for singly charged ions by the ion trap. Multiply charged ions were not detected until now. A mass spectrum of singly charged β-Endorphin (M = 3464.98 g/mol) is shown in the Supplementary Fig. 3. The highest m/z value measured so far with LAMMA 2000 under high focusing conditions was about 17,600 for the single charged molecular ion of Myoglobin (unpublished data). Insulin (M = 5807.57 g/mol) can be easily detected under high focusing condition as described earlier [23,24]. Due to detector limitations, detection of large proteins with LAMMA 2000 is currently not possible. We have no indication that a mechanistical mass limit exists which is connected to the focus size. It appears instead that there are no radical changes in desorption/ionization mechanism when going to small laser spot sizes. It is demonstrated in this paper that the behavior of ion formation is rather similar and follows a gradual trend when changing spot sizes. This is in contrast to the conclusion of the thermal desorption model when employed with the published fit parameters, excluding a functionable desorption/ionization regime at spot sizes in the range of 1 μm [11].

5. Conclusions

Characteristic laser beam parameters in high lateral resolution MALDI imaging mass spectrometry were determined under well-defined conditions. It was demonstrated that both tested setups have an optical resolution below 10 μm in diameter at the focal point of the laser beam. The behaviour of the two instruments with respect to ion formation was investigated. It was demonstrated that the dependence of ion signal intensities on laser fluence is in accordance with the behaviour described for larger spot sizes when extrapolated to the micrometer regime. Slopes of the ion signal versus fluence curve and the dynamic range of the observed ion signal intensities were found to be smaller than those found for larger laser spots, as expected. These results argue for a general mechanism of ion formation for large and small laser spot sizes with no radical changes below a certain spot size limit but gradual trends with spot size.

Acknowledgements

Financial support by the European Union (STREP project No. 518194), by the Bundesministerium für Bildung und Forschung BMBF (NGFN, project No. 0313442) and by the Deutsche Forschungsgemeinschaft DFG (project Sp 314/10-1) is gratefully acknowledged. This publication represents a component of the doctoral (Dr. rer. nat.) thesis of S.G. at the Faculty of Biology and Chemistry, Justus Liebig University Giessen, Germany.

Appendix A. Supplementary data

Supplementary data associated with this article can be found, in the online version, at doi:10.1016/j.ijms.2010.03.014.

References

[1] M. Karas, F. Hillenkamp, Laser desorption ionization of proteins with molecular masses exceeding 10,000 daltons, Analytical Chemistry 60 (20) (1988) 2299–2301.
[2] M. Karas, D. Bachmann, U. Bahr, F. Hillenkamp, Matrix-assisted ultraviolet laser desorption of non-volatile compounds, International Journal of Mass Spectrometry and Ion Processes 78 (1987) 53–68.
[3] M. Karas, D. Bachmann, F. Hillenkamp, Influence of the wavelength in high-irradiance ultraviolet laser desorption mass spectrometry of organic molecules, Analytical Chemistry 57 (14) (1985) 2935–2939.
[4] M. Karas, U. Bahr, Laser desorption mass spectrometry, TrAC Trends in Analytical Chemistry 5 (4) (1986) 90–93.
[5] B. Spengler, M. Hubert, R. Kaufmann, MALDI ion imaging and biological ion imaging with a new scanning UV-laser microprobe, in: Proceedings of the 42nd Annual Conference on Mass Spectrometry and Allied Topics, Chicago, Illinois, May 19–June 3, 1994, p. 1041.
[6] B. Spengler, M. Hubert, Scanning microprobe matrix-assisted laser desorption ionization (SMALDI) mass spectrometry: instrumentation for sub-micrometer resolved LDI and MALDI surface analysis, Journal of the American Society for Mass Spectrometry 13 (6) (2002) 735–748.
[7] D.A. Allwood, R.W. Dreyfus, I.K. Perera, P.E. Dyer, Optical absorption of matrix compounds for laser-induced desorption and ionization (MALDI), Applied Surface Science 110 (1997) 154–157.
[8] V. Horneffer, K. Dreisewerd, H.C. Lüdemann, F. Hillenkamp, M. Läge, K. Strupat, Is the incorporation of analytes into matrix crystals a prerequisite for matrix-assisted laser desorption/ionization mass spectrometry? A study of five positional isomers of dihydroxybenzoic acid, International Journal of Mass Spectrometry 185/186/187 (1999) 859–870.
[9] R.C. Beavis, B.T. Chait, K.G. Standing, Factors affecting the ultraviolet laser desorption of proteins, Rapid Communications in Mass Spectrometry 3 (7) (1989) 233–237.
[10] B. Spengler, M. Karas, U. Bahr, F. Hillenkamp, Excimer laser desorption mass spectrometry of biomolecules at 248 and 193 nm, Journal of Physical Chemistry 91 (26) (1987) 6502–6506.
[11] K. Dreisewerd, M. Schürenberg, M. Karas, F. Hillenkamp, Influence of the laser intensity and spot size on the desorption of molecules and ions in matrix-assisted laser desorption/ionization with a uniform beam profile, International Journal of Mass Spectrometry and Ion Processes 141 (2) (1995) 127–148.
[12] H. Qiao, V. Spicer, W. Ens, The effect of laser profile, fluence, and spot size on sensitivity in orthogonal-injection matrix-assisted laser desorption/ionization time-of-flight mass spectrometry, Rapid Communications in Mass Spectrometry 22 (18) (2008) 2779–2790.
[13] G. Westmacott, W. Ens, F. Hillenkamp, K. Dreisewerd, M. Schürenberg, The influence of laser fluence on ion yield in matrix-assisted laser desorption ionization mass spectrometry, International Journal of Mass Spectrometry 221 (1) (2002) 67–81.
[14] A. Ingendoh, M. Karas, F. Killenkamp, U. Giessmann, Factors affecting the resolution in matrix-assited laser desorption–ionization mass spectrometry, International Journal of Mass Spectrometry and Ion Processes 131 (1994) 345–354.
[15] B. Spengler, U. Bahr, M. Karas, F. Hillenkamp, Postionization of laser-desorbed organic and inorganic compounds in a time of flight mass spectrometer, Analytical Instrumentation 17 (1–2) (1988) 173–193.

[16] K. Dreisewerd, M. Schürenberg, M. Karas, F. Hillenkamp, Matrix-assisted laser desorption/ionization with nitrogen lasers of different pulse widths, International Journal of Mass Spectrometry and Ion Processes 154 (3) (1996) 171–178.
[17] C. Menzel, K. Dreisewerd, S. Berkenkamp, F. Hillenkamp, The role of the laser pulse duration in infrared matrix-assisted laser desorption/ionization mass spectrometry, Journal of the American Society for Mass Spectrometry 13 (8) (2002) 975–984.
[18] B. Spengler, ULISSES Data Acquisition Software Package, 8.21 ed., 1985–2009.
[19] M. Koestler, D. Kirsch, A. Hester, A. Leisner, S. Guenther, B. Spengler, A high-resolution scanning microprobe matrix-assisted laser desorption/ionization ion source for imaging analysis on an ion trap/Fourier transform ion cyclotron resonance mass spectrometer, Rapid Communications in Mass Spectrometry 22 (20) (2008) 3275–3285.
[20] B. Spengler, V. Bökelmann, Angular and time resolved intensity distributions of laser-desorbed matrix ions, in: Symp on Fundamental Processes in Sputtering of Atoms and Molecules, on the Occasion of the 250th Anniversary of the Royal Academy of Science and Letters, Copenhagen, Denmark, 1992, pp. 379-385.
[21] V. Bökelmann, B. Spengler, R. Kaufmann, Dynamical parameters of ion ejection and ion formation in matrix-assisted laser desorption/ionization, European Mass Spectrometry 1 (1) (1995) 81–93.
[22] A.E. Siegman, Laser: University Science Books, 1986.
[23] W. Bouschen, B. Spengler, Artifacts of MALDI sample preparation investigated by high-resolution scanning microprobe matrix-assisted laser desorption/ionization (SMALDI) imaging mass spectrometry, International Journal of Mass Spectrometry 266 (1–3) (2007) 129–137.
[24] W. Bouschen, O. Schulz, D. Eikel, B. Spengler, Matrix vapor deposition/recrystallization and dedicated spray preparation for high-resolution scanning microprobe matrix-assisted laser desorption/ionization imaging mass spectrometry (SMALDI-MS) of tissue and single cells, Rapid Communication in Mass Spectrometry 24 (3) (2010) 355–364.
[25] L.V. Zhigilei, Y.G. Yingling, T.E. Itina, T.A. Schoolcraft, B.J. Garrison, Molecular dynamics simulations of matrix-assisted laser desorption – connections to experiment, International Journal of Mass Spectrometry 226 (1) (2003) 85–106.
[26] P. Demirev, A. Westman, C.T. Reimann, P. Hakansson, D. Barofsky, B.U.R. Sundqvist, Y.D. Cheng, W. Seibt, K. Siegbahn, Matrix-assisted laser desorption with ultra-short laser-pulses, Rapid Communications in Mass Spectrometry 6 (3) (1992) 187–191.
[27] P.Y. Yau, T.W.D. Chan, P.G. Cullis, A.W. Colburn, P.J. Derrick, Threshold fluences for production of positive and negative ions in matrix-assisted laser desorption/ionisation using liquid and solid matrices, Chemical Physics Letters 202 (1–2) (1993) 93–100.
[28] W. Ens, Y. Mao, F. Mayer, G. SK, Properties of matrix-assisted laser desorption. Measurements with a time-to-digital converter, Rapid Communications in Mass Spectrometry 5 (3) (1991) 117–123.
[29] V.V. Laiko, M.A. Baldwin, A.L. Burlingame, Atmospheric pressure matrix assisted laser desorption/ionization mass spectrometry, Analytical Chemistry 72 (4) (2000) 652–657.
[30] V.M. Doroshenko, V.V. Laiko, N.I. Taranenko, V.D. Berkout, H.S. Lee, Recent developments in atmospheric pressure MALDI mass spectrometry, International Journal of Mass Spectrometry 221 (1) (2002) 39–58.
[31] P. Chaurand, K.E. Schriver, R.M. Caprioli, Instrument design and characterization for high resolution MALDI-MS imaging of tissue sections, Journal of Mass Spectrometry 42 (4) (2007) 476–489.